A New Field Test for Highway Shoulder Permeability

IURY L. MAYTIN,
Highway Research Section, Division of Industrial Research, Washington State University, Pullman, Wash.

Many pavement failures can be traced to a loss of support by the roadbed. This condition is often the result of inadequate drainage through highway shoulders that lose their desired permeability when water becomes trapped beneath the pavement. This paper presents a new method of testing the drainage of highway shoulders in the field. The test is rapid and enables the operator to observe visually the advance of a saturated moisture front throughout a shoulder cross-section by noting the lighting sequence of small neon bulbs arranged in a grid on a panel. These bulbs are electrically connected to steel probes driven into the shoulder at intervals along its width. The test and the equipment were developed with a full-scale laboratory model of a highway shoulder, using various gradations as the single variable. Special graphs were plotted to enable an operator to get a general idea of the permeability of the material in a very short time while the test is in progress. The field tests show good agreement with the laboratory data. Further field work is under way on major highways in several parts of the State of Washington.

• WHEN a granular base course is built to support traffic as well as to drain, it must remain open-graded throughout the pavement life. Considerable subgrade intrusion may occur if free water is present in the base (*1*).

Drainage must be adequate to lower permanently the ground water table to an acceptable depth below the pavement surface (*2*). If the granular subbase does not extend to the ditch line or if the material becomes clogged with fines, water may be trapped and prevented from flowing laterally. This condition causes a partial or total loss of stability that ultimately produces pavement failure.

This paper presents a new approach to the problem of evaluating in the field the ability of a highway shoulder to drain. The new test gives a rapid evaluation of relative permeability with a minimum of disturbance to material and traffic. It analyzes the entire shoulder cross-section rather than localized samples which are not necessarily representative. The test classifies drainage characteristics into categories of permeability that are excellent, acceptable, borderline, and unsuitable. When the data show that a road section cannot drain water at a suitable rate, the area may be subjected to more detailed tests. These should

include mechanical analyses and field densities of representative samples.

BASIC TEST

The test equipment consists of a water supply, a perforated water injection pipe, several steel probes, connecting cables, and an observation panel (Fig. 1). The position of a moisture front is indicated on the panel when the water short circuits electrodes in probes that have been driven into the highway shoulder. The electrical shorting of each electrode lights a corresponding neon bulb on the panel (shown as solid black circles). An operator is thus able to "see" the shape and the rate of advance of the water envelope. The dotted line drawn through or directly above the glowing neons approximates the surface and depth of the saturated material.

Figure 2 shows the detection of a case of partial "plugging" within a highway shoulder. Water does not flow as quickly through the clogged areas as through the surrounding material. The timed lighting sequence of the neons shows this.

This new test was developed in a full-scale laboratory model of a highway shoulder. Objectives of this model (described in Appendix A) were the following:

1. To determine a permeability standard for an index of relative permeability.

2. To establish a compaction routine insuring uniformity of test conditions.

3. To compare drainage in highway base courses and shoulders with

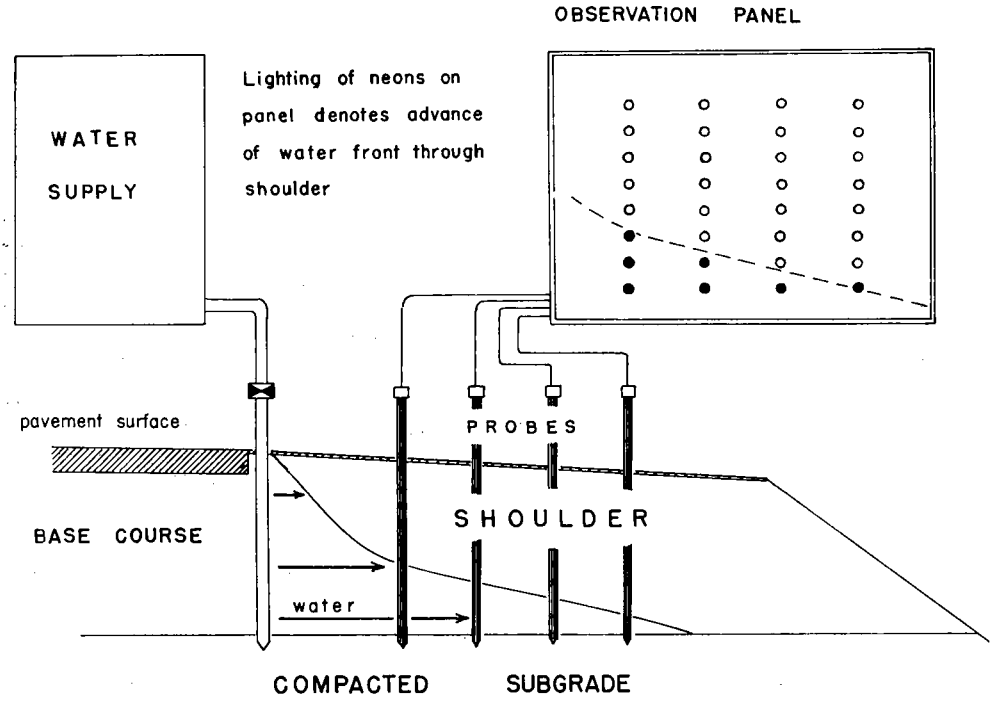

Figure 1. Simplified sketch of test and equipment.

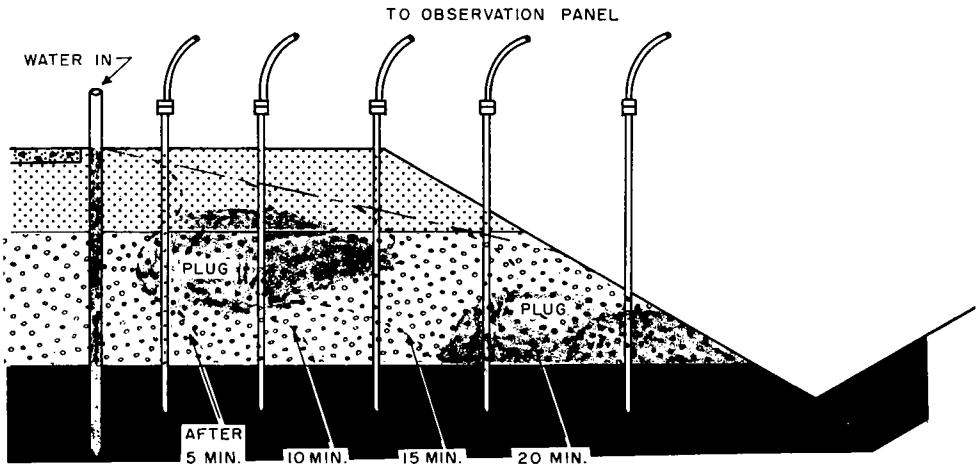

Figure 2. Diagram showing effect of shoulder "plugging" on advancing water front.

drainage in a model consisting of similar material.

4. To study the type of correlation applicable to laboratory model and field conditions.

FIELD TEST PROCEDURES

Setting up the equipment is simple. The perforated water injection pipe and probes are driven into the highway material. The protective caps are removed, and the probes are cable-connected to the observation panel. An alternating current is then introduced into the entire circuit. Direct current should not be used because of polarization. The test begins and is timed from the moment water flows in the injection pipe. The water level in the pipe must be held constant throughout the test to avoid misleading and inaccurate data. All data in this report were recorded from tests made with water in the injection pipe under atmospheric pressure at ground surface level.

If a field test is to be practical, it must quickly bracket the degree of permeability of base course or shoulder material. The amount of time taken to complete a test can be shortened considerably by the proper choice of spacing between the probes and the injection pipe. This calls for an educated guess, based on observation of the material and knowledge of its characteristics. For example, an open-graded base course may be expected to pass water at a velocity of 1 to 5 ft per min, whereas another one with more fines might show velocities of only a few hundredths of a foot per minute. As will be shown later, a definite relation exists between velocity and the amount of fines in a compacted material. The operator need only have a rough idea of the graduation in order to estimate the probable range of velocity and, consequently, to know how far to space his probes.

The probes must be driven through the entire depth of the course whose drainage is to be studied. It is important to have the lowest electrode on each probe imbedded into the sub-

grade material. Failure to observe this may result in misleading observations, because water can flow over the relatively impervious subgrade but underneath the lowest electrode. It is also possible for water to flow downward at a faster rate than outward. Whether this is due to high vertical permeability or to channeling from internal cracks, the situation produces no neon lighting. The problem can easily be recognized if the operator keeps track of his water input in the material.

DATA INTERPRETATION

Analysis of test results indicates a satisfactory correlation between velocity, relative permeability, and the amount of fines in the material.

Tables 1 and 2 summarize the basic information gathered from tests performed in the model and on the highways. Series I, II, and III were tests done on the same model shoulder using 5/8 in. minus crushed basalt. After completion of a test series, the material was removed from the

TABLE 1
SUMMARY OF DATA, LABORATORY AND FIELD TESTS [1]

Test Series	% Passing Sieve No. 40	% Passing Sieve No. 80	% Passing Sieve No. 200	$\overline{V}_s$ (ft/min)	$\overline{V}_d$ (ft/min)	γ Dry (pcf)	K_s (ft/min)	K_d (ft/min)	K_{f30} (ft/min)
Lab:									
I	3	2	1	0.40	1.5	127	4.8	16.7	0.16
II	8	4	2	0.08	0.30	122	0.72	2.6	0.027
III	18	10	5	0.04	0.13	127	0.33	1.1	0.013
Field:									
A	4	2	1	—	1.5	121	—	—	0.15
B	7	5	3	—	0.4	131	—	—	0.029
C	16	11	9	—	0.15	138	—	—	0.014
D	37	24	17	—	0.03	141	—	—	0.000 [2]

[1] V_s=velocity of water within aggregates, taken below stabilized slope of water envelope; V_d=velocity of advancing front of water; K_s = permeability (from V_s/S in which S = slope of water envelope); K_d = permeability (from V_d/S); K_{f30} = permeability (from falling head permeameter after 30-min saturation).

[2] Permeabilities between 0.00004 and 0.001 ft/min indicate possible experimental errors.

TABLE 2
COMPARISON OF VELOCITY, DENSITY, AND GRADATION, FIELD TESTS

Test Series	V (ft/min) [1]	γ Dry (pcf)	5/8-Minus Fraction of Sample (% passing) 1/4-In.	No. 10	No. 20	No. 40	No. 80	No. 200	K (ft/min) [2]
D	0.025–0.045	141	—	—	—	37	24	17	0.2–0.4
B	0.1–0.2	138	58	28	20	16	11	9	1–2
C	0.3–1.0	131	43	17	10	7	5	3	3–6
A_1	0.6–1.2	122	41	20	11	7	3	3	6–12
A_2	1.2–2.5	121	34	12	6	4	2	1	12–25
A_3	1.1–2.0	118	26	10	7	4	2	1	11–20

[1] Measured from 1 to 2 ft up from shoulder break to 1 ft past shoulder break.

[2] Computed on premise if materials containing similar fractions of minus 40 fines exhibit same velocities and permeameter values, then slope of water flowing through these materials is also similar.

flume, remixed with added fines and recompacted. Permeability was computed from the general Darcy equation in two ways: (a) using dynamic velocity, and (b) using velocity of water within the saturated material after flow conditions had reached stability. Dynamic velocity is defined in this paper as the velocity of the foremost edge, or toe, of a water envelope moving into relatively dry shoulder or base course material. Model test results show that dynamic velocity is approximately 3.1 times as great as the velocity measured with stabilized flow conditions.

The two types of velocities were studied to determine if the dynamic velocity could ultimately be used in the field, because it is observed quickly and easily without additional equipment. Data show that this is possible, because the two velocities are related by a constant.

Observation of velocity within a saturated material, or a fluid within a fluid, was done successfully with a special technique. This consists of the injection of a strong saline solution to the water feeder pipe, and the timing of the passage of its front by noting the sudden illumination of a

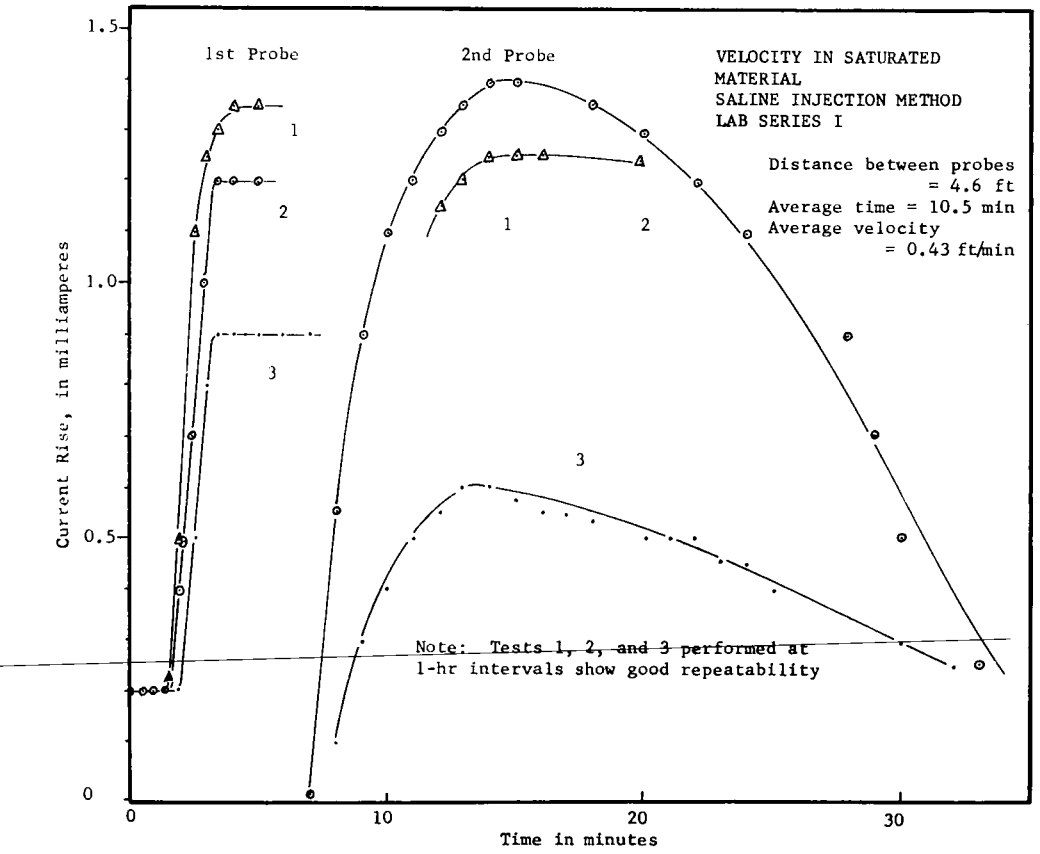

Figure 3. Electrode current vs time.

neon bulb or by plotting a graph of electrode current vs time. Figure 3 shows three typical time-current curves for Series I. Although this technique calls for more skill than field crews may possess, there seems to be little need for this method because use of the dynamic velocity gives results that are reliable enough. By adding salt to the water, the test can be conducted in rainy weather or with a roadbed already saturated. This increases the usefulness of this new test.

Figure 4 presents one of the significant results of the model tests: the agreement between permeabilities obtained in the model and permeabilities recorded from permeameter tests. These values are plotted as a function of the amount of fines in the material.

For each gradation, permeability was calculated in the model from observed velocity and slope, using Darcy's general equation for laminar flow, $K = \frac{V}{S}$. The material for each of the three test series was also recompacted in cylindrical molds at corresponding densities and subjected to a falling head permeameter tests. The resulting permeabilities were calculated from the equation $K = \frac{aL}{A\Delta t} \log_{10} \frac{h_0}{h_1}$. The two graphs are parallel, which indicates the linear relationship, hence the excellent correlation between the two methods.

The dotted vertical lines for the three test series are bandwidths containing the data scatter of all the permeabilities obtained. Each point inscribed by a circle represents a mean value. Thus each bandwidth

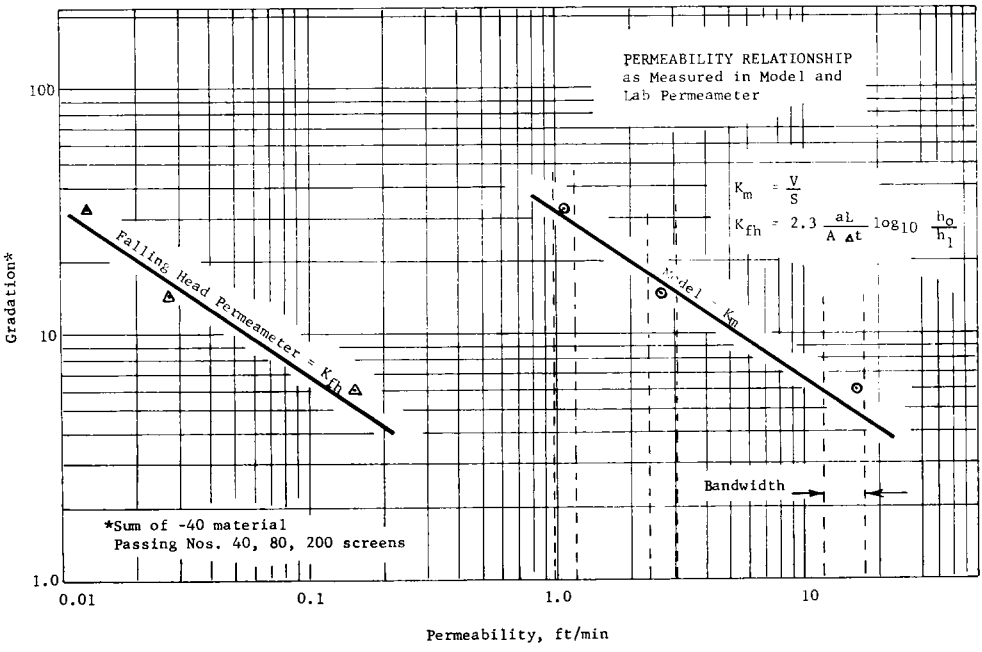

Figure 4. Permeability vs gradation.

serves as an index for estimating the relative accuracy of any one test in the model.

Table 3 gives typical data for the coarsest gradation (Series I) compacted in the model. It illustrates how the permeability bandwidth for Figure 4 depends on the maximum and minimum values of slope observed in the 8 tests listed, or 0.015 and 0.085, respectively. When divided into the virtually constant value of velocity (under stabilized flow) the corresponding permeabilities are 4.1 and 5.1 ft per min. Using dynamic velocities, the maximum and minimum permeabilities are 11.4 and 18.9 ft per min, respectively.

The velocity of a water front through highway shoulders can show a variety of patterns, as shown in Figure 5. In some cases, velocities are several times higher when measured 1 ft from the injection pipe than when observed 2, 3, and 4 ft away. In other instances, practically no velocity change is observed at any distance between injection pipe and the

TABLE 3
MODEL DATA FOR TEST SERIES I[1]

Test No.	S	K (ft/min)	V_s (ft/min)	V_d (ft/min)	$\frac{V_d}{V_s}$
1	—	—	—	—	—
2	0.085	5.0	0.43	1.2	2.7
3	0.085	5.1	0.43	1.4	3.1
4	0.094	4.6	0.42	1.6	3.5
5	0.086	5.0	—	—	—
6	0.082	5.2	0.43	1.5	3.2
7	0.105	4.1	0.42	1.5	3.2
8	0.089	4.8	0.44	1.4	3.0
Avg.	0.090	4.8	0.43	1.5	3.1

[1] S = measured stabilized slope of water envelope; K = Permeability measured from $\frac{V_s}{S}$; V_s = velocity of water below stabilized slope of water envelope at $\frac{1}{3}$ depth; V_d = velocity of advancing water front, referred to as dynamic velocity.

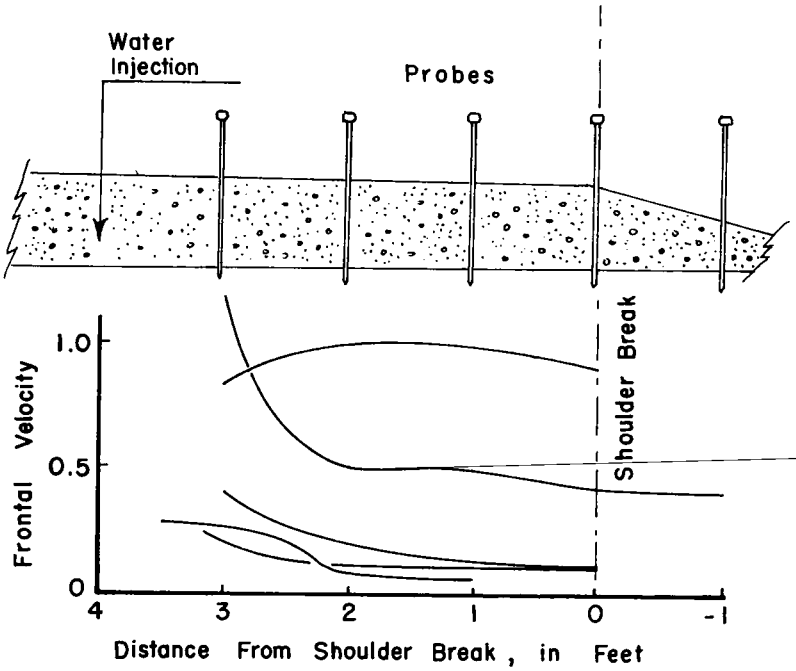

Figure 5. Typical velocity profiles in highway shoulders.

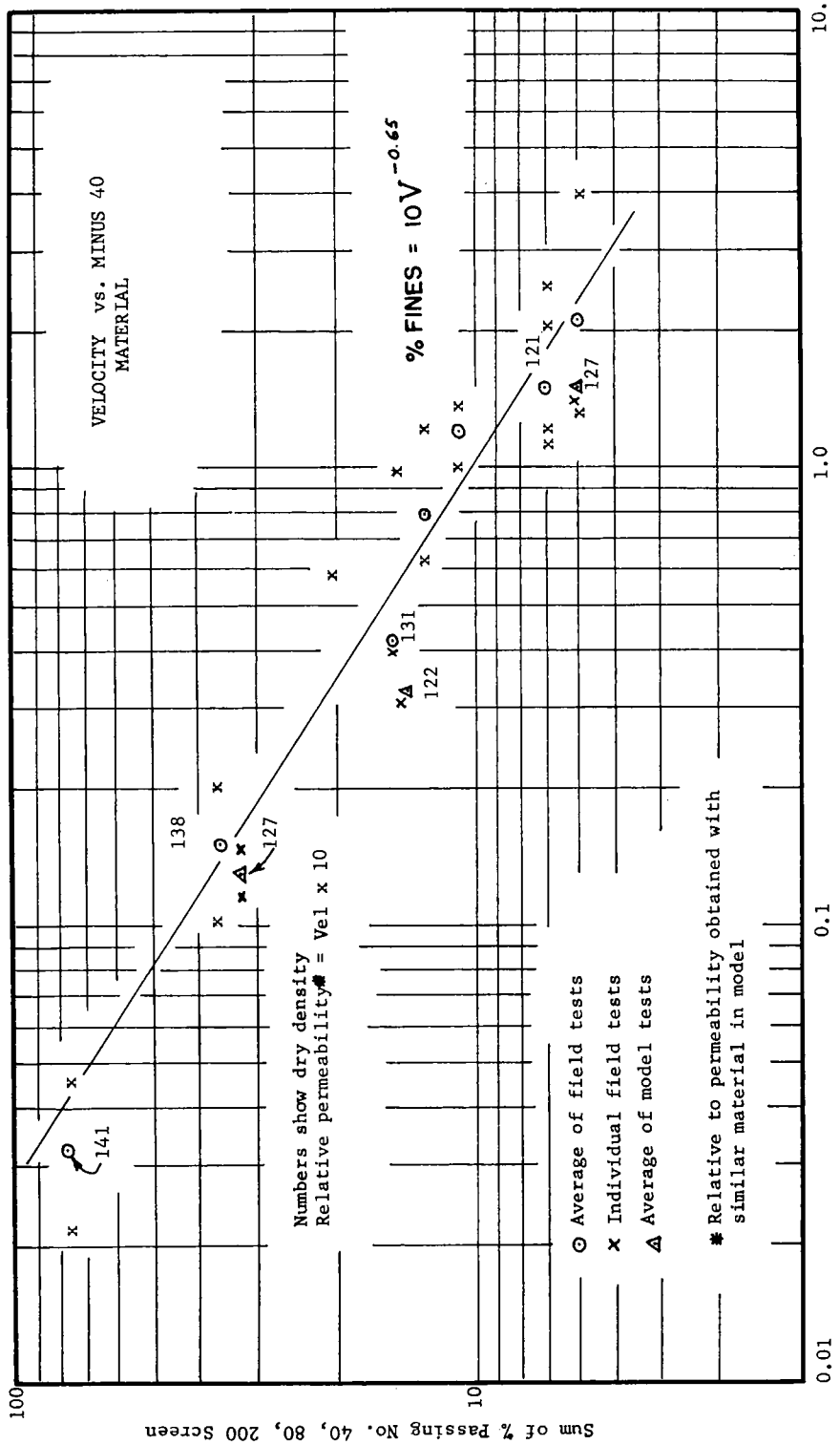

Figure 6. Relationship of fines to velocity.

furthest probe, which may or may not be past the "break" in shoulder slope. These velocity patterns may be partly the result of subgrade geometry which could produce flow conditions ranging from three-dimensional to two-dimensional. Cracks and poorly graded material could also influence the velocity pattern.

In practice, a satisfactory and representative average velocity can be obtained if readings are taken at least 1.5 ft away from the injection pipe.

Velocity is a practical index for determining drainage characteristics in the model and on the highways. This is shown in Figure 6, where it has been plotted as a function of the sum of minus 40 material passing Nos. 40, 80, and 200 screens. Observed velocities in the field are changed to relative permeabilities simply by multiplying by 10. This is legitimate because slopes observed for the three different gradations in the model were in the order of 0.1. Slight deviations have negligible effects on the permeability. For all practical purposes, the slope may be treated as 0.1 without introducing significant errors. It can therefore be stated that $K = 10V$ when model and highway tests are performed identically.

ANALYSIS

Interpretation of data from experiments on permeability—relative density—D_{10} relations conducted by Kane (*3*) and Burmister (*4*) shows that for material with D_{10} values similar to those of the flume model gradations, increasing the relative density from 50 to 90 percent causes the permeability to drop by a factor of 2 to 3. This is far less significant than the 15-fold decrease in permeability observed with model test Series I and III when the amount of fines was increased 5 times. In practice, the relative density of a highway base course or shoulder deviates little from a mean value, although intrusion of fines may raise the percentage of minus 40 material several fold. Figure 7 is a dimensionless graph

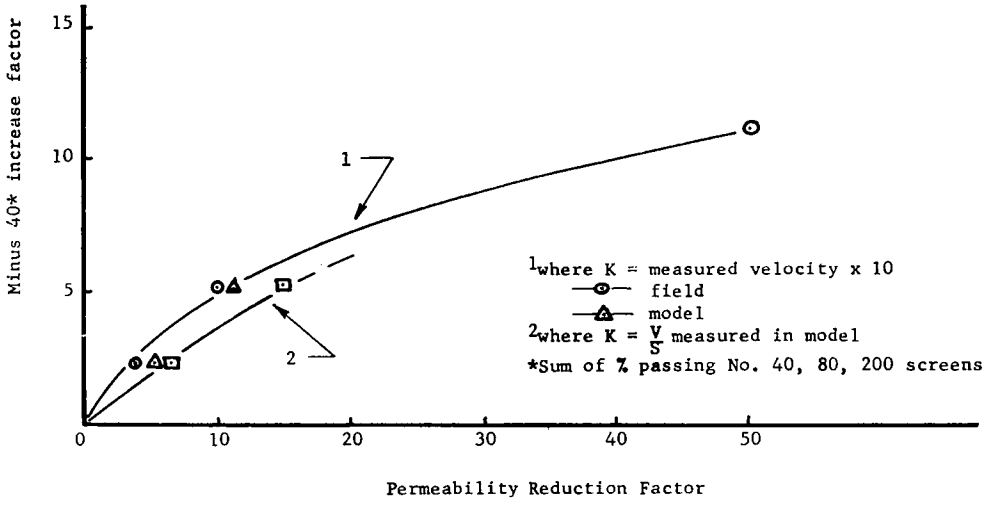

Figure 7. Effect of increasing contents of fines on permeability.

showing that the permeability reduction factor is not a constant in relation to the sum of fines passing Nos. 40, 80, and 200 screens.

The results of single permeameter tests on loose material are often misleading. Difficulties in sampling and in reproducing field conditions in the laboratory may lead to large errors. Many tests are needed. Permeability tests are subject to certain experimental errors (*5*) such as may arise when a filter skin of fine material forms on the surface of the sample, or air bubbles block the voids and reduce the permeability. The data for Series D field tests may reflect such experimental errors. The discrepancies in values observed invalidate the practical value of permeameter tests for materials with high percentages of fines. For the coarser gradations, such a test was useful in establishing the relationship between velocity and permeability, as calculated by the electric probe test method. In the field, however, information on the graduation of fines is simpler to obtain than permeameter test data, and it provides reliable index of permeability. Figures 8 and 9 show the gradation of the materials tested in the model and on the highways.

There has been much investigation made to obtain the value of K in Darcy's $V=KS$. Hazen (*6*) related it to the effective size of the material (D_{10}) which is the grain size shown by mechanical analysis to be smaller than 90 percent of the material. Laboratory permeability tests have been devised for different materials (*7*).

Examination of actual road sections sometimes reveals pronounced and erratic segregation of particle size. It is therefore realistic to visualize that as water seeps outward underneath the pavement and through the shoulder material, the flow may alternately shift from laminar to turbulent conditions. Only the steady state of flow through material fully saturated can be analyzed with precision (*8*). Another type of complex flow occurs below a temporarily elevated ground water level or free water surface having various degrees of saturation and air clogging of the voids. A good example of this is the flow of water through a base course beneath a pavement during rainy periods.

This new test is designed to indicate over-all drainage within a granular complex. The degree of precision need not be as critical as for situations requiring detailed analysis through special laboratory tests. Data show that in the model, flow was essentially laminar for the three gradations tested. It might be interesting from an academic standpoint to observe the velocity-slope relationship for a coarse, open-graded material through which the flow would be in the turbulent range. However, inasmuch as this test is designed primarily for use on highways, such study would not be of immediate importance.

Special pumping tests for the horizontal permeability of various undisturbed sand layers (*9*) in the alluvial valley of the Mississippi River showed a definite relationship between the effective grain size, D_{10}, and horizontal permeability. Table 1 indicates such a correlation between the minus 40 fractions and permeability.

Some decision must be made on the choice of permeability ranges for classifying the drainage capacity of the material under test. In effect, these ranges will represent a set of standards. Whether the test is used

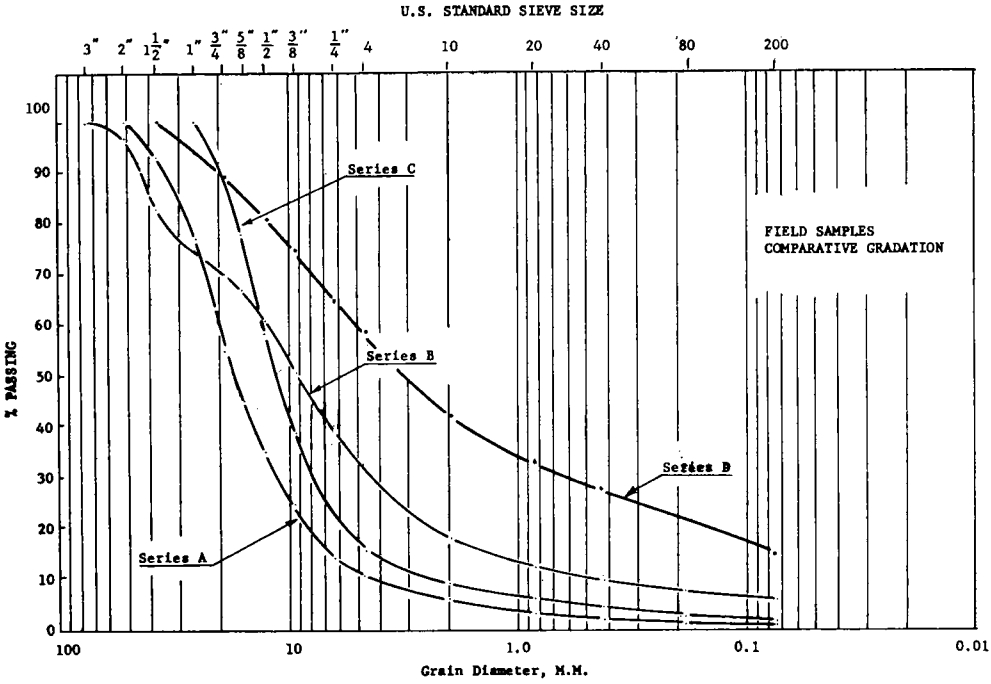

Figure 8. Mechanical analysis of field tests.

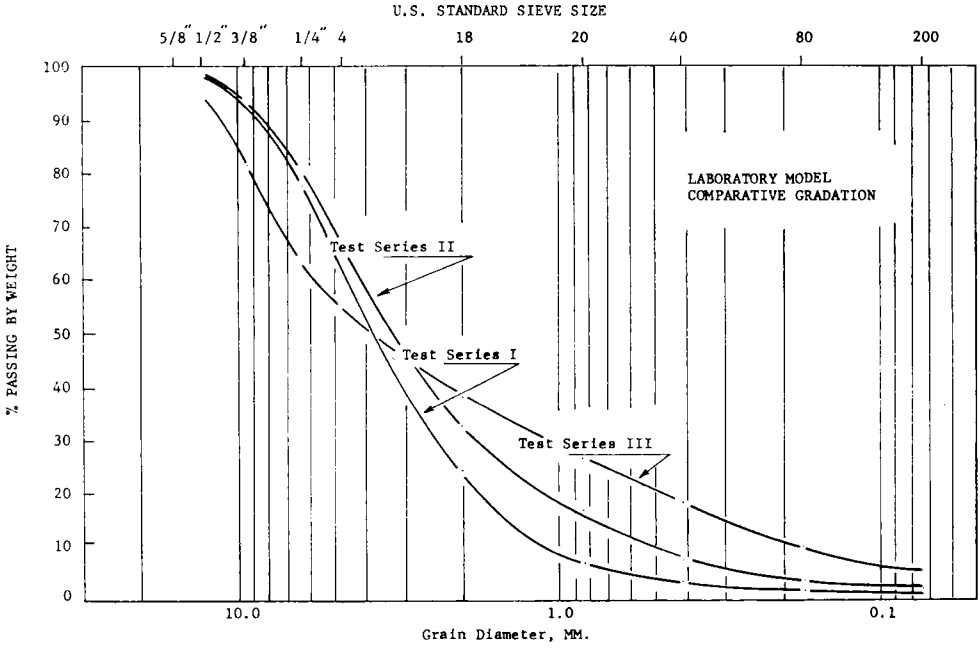

Figure 9. Mechanical analysis of model tests.

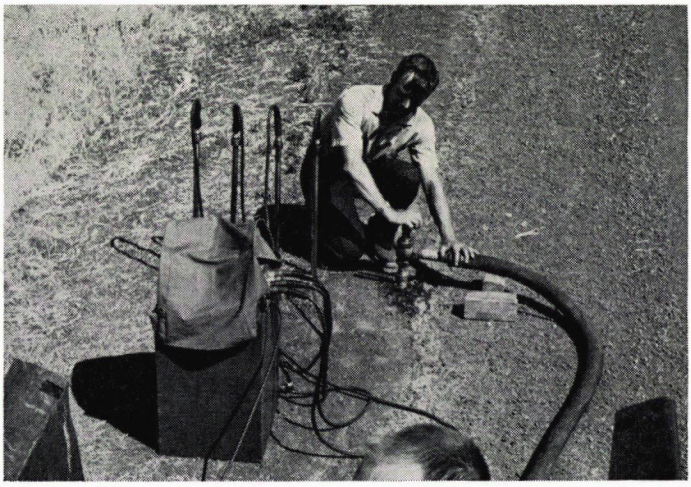

Figure 10. Highway shoulder under test.

to check drainage on a highway construction project, or on existing roads, as shown in Figure 10, the operator must be able to decide right then and there whether to extract samples for further investigation.

CONCLUSIONS

This new test is practical for classifying drainage into such categories as excellent, acceptable, questionable, and bad. These are suggested ratings whose permeability limits remain to be established after additional studies to relate cause and effect of pavement distress, or by the agency adopting this new test.

Studies made in a full-scale laboratory model shoulder and on actual highways indicate permeability can be correlated to the observed water velocity with an accuracy level satisfying the main objective of this field test. Preliminary tests indicate this electric probe method should prove of substantial benefit in highway maintenance. The equipment is easily transported and can be handled by semiskilled personnel with less risk of collecting in-

accurate data than with the use of laboratory permeameter tests.

REFERENCES

1. YODER, E. J., "Principles of Pavement Design." Wiley (1959).
2. NOBLE, C. M., "Increasing the Load-Carrying Capacities of Subgrade." *Trans. ASCE,* Vol. 121 (1956).
3. KANE, H., "Investigation of the Permeability Characteristics of Sands." MS thesis. Columbia Univ. (1948).
4. BURMISTER, D. M., "The Importance and Practical Use of Relative Density in Soil Mechanics." *Proc. HSTM,* vol. 48 (1948).
5. PECK, HANSON, AND THORNBURN, "Foundation Engineering." Wiley (1953).
6. HAZEN, A., "Some Physical Properties of Sands and Gravels." 24th Annual Report, Mass. State Board of Health (1892-1893).
7. STEARNS, N. D., "Laboratory Tests on Physical Properties of Water Bearing Materials." U.S. Geol. Survey Water Supply Paper 596-F (1927).
8. BURMISTER, D. M., "Principles of Permeability Testing of Soils." Symposium on Permeability of Soils, ASTM Special Tech. Publ. 163 (1954).
9. MANSUR, C. L., "Laboratory and In-Situ Permeability of Sand." *Trans. ASCE,* vol. 123 (1958).

APPENDIX A

Laboratory Model

The 16-ft wood flume had 4-ft side walls braced with buttresses bolted to the frame, as shown in Figure 11. The maximum lateral deflection recorded anywhere along the side walls was $\frac{1}{16}$ in. The concrete floor precluded any deflections in the horizontal alignment of the floor deck on the model.

Because the depth of existing base courses and shoulders seldom exceeds 24 in., the flume was designed for this depth. The 16-ft length allowed testing a full width shoulder section while retaining several feet of clearance between the end bulkhead and the water injection pipe. During the entire testing program, this distance was kept at 4 ft, which proved adequate to minimize back-pooling and possible interference with flow patterns occurring downstream from the point of water injection. It is possible that flow characteristics were defined to some degree by side walls effect. However, because all tests were performed identically in the same flume, this possible variable is treated as an unknown constant.

The roller-vibrator compactor (shown in Fig. 12) has dual 8-in. ribbed steel rollers having $\frac{1}{4}$-in. clearance to the walls of the model and mounted on a rectangular steel frame. A pneumatic tamper bolted to the deck of the frame transmits vertical vibrations to the rollers. During compaction, the frequency was approximately 15 cycles per sec which appeared to be the resonance of the

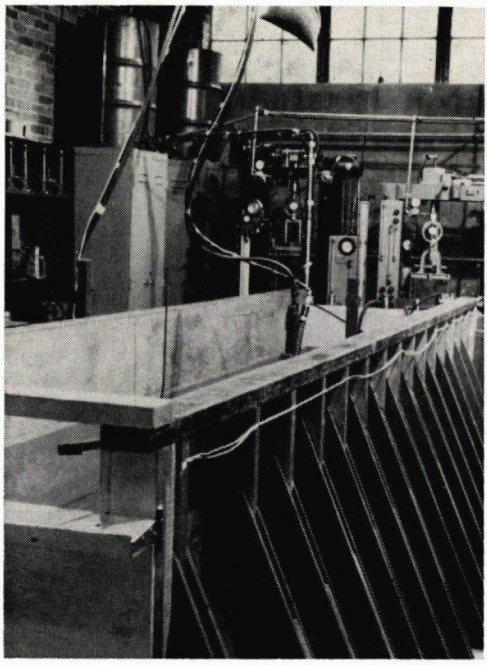

Figure 11. Flume used in model tests.

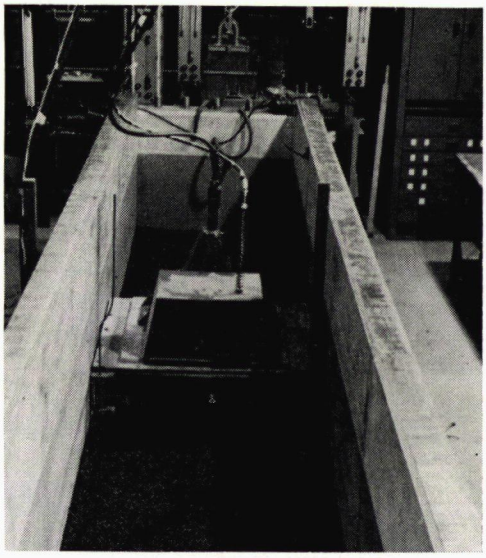

Figure 12. Compactor in flume.

400-lb compactor. A ⅓-hp electric motor supplied power to a reduction gear box and chain drive, propelling the unit at 1 ft per sec. The flume automatically reverses when triggered by an antenna atop the compactor. Safety stop switches located behind the reversing switches cut off electric power if the compactor overrides the reversing mechanism.

Compaction Procedure

The aggregate material for all laboratory tests was compacted in ½-in. layers to a depth of 24 in. Each layer was rolled at a moisture content of 5 to 6 percent. The crushed basalt used in all the laboratory tests came from a stockpile of material for road construction and maintenance work. Twenty passes a layer produced a compactive effort within the range of measured field densities.

The thin-layered compaction routine formed a uniformly graded and homogeneous deep blanket of material. The maximum density deviation for repeated tests taken along the length and depth of the model was 1.5 lb per cu ft in Series III and 1.0 lb per cu ft in Series I and II. The Washington State Department of Highways densometer was used for all in-place density tests in the model and in the field.

Instrumentation

The electrical monitoring system consists of (a) a source of AC power, (b) an observation and control box, (c) probe assemblies, and (d) interconnecting cables and sockets.

The AC power must supply at least 110 volts to ignite the miniature neon bulb. Wattage rating is determined by the total number of neon bulbs on the observation panel. A vibrator power supply with a 12-volt DC input

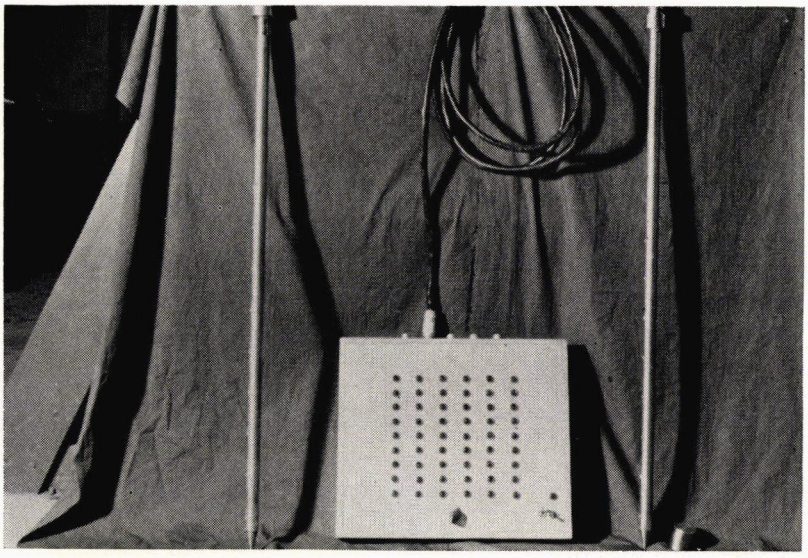

Figure 13. Observation panel and associated equipment.

and 110-volt AC output at 15 watts was used in the field.

The probes used for all tests were 7/8-in. outside diameter steel pipes fitted with a solid steel point at the lower end and a special cap at the upper, or driving, end. The cap slipped over an amphenol socket and rested on the heavy steel collar welded to the probe. It protected the delicate amphenol socket from injury during transit and repeated sledge hammer blows.

Small, evenly-spaced holes were bored through one side of the probe. An insulated wire was centered within each hole and connected electrically to a pin in the socket. Each hole then was filled with an epoxy glue which, after hardening, was filed and contoured flush with the outer surface of the probe. These were the electrodes. The epoxy was not allowed to soften or absorb water. If the epoxy does not possess a high dielectric constant, it may short circuit the electrical potential between the center wire and the grounded steel body of the probe. This would ignite the neon bulb.

The control box, or observation panel, had as many vertical rows of neon bulbs as there were probes. Each vertical row, cabled and connected to a probe, had as many neon bulbs as there were electrodes in each probe. The entire system was grounded through an internal grounding wire as well as through the outer shield of the cable bundle. The wiring circuit was such that shorting any electrode caused the corresponding neon to light on the panel. Figure 13 shows observation panel with two probes and one of the cables.

APPENDIX B

Correlation of Model and Field Data

In Darcy's equation,

$$K_m = \frac{V}{S_m} \qquad (1)$$

The model's equation from collected data is

$$K = \frac{V_m}{S} \qquad (2)$$

In the model and in the field, courses with similar fractions of minus 40 material show similar velocities, or

$$V_m \cong V_f \qquad (3)$$

In the model and in the field, samples from courses with similar fractions of minus 40 material show similar permeabilities with the laboratory permeameter (see Table 1), or

$$K_m' \cong K_f' \qquad (4)$$

It follows from Eqs. 2, 3, and 4 that

$$\frac{K_m' S_m}{V_m} \cong \frac{K_f' S_f}{V_f} \qquad (5a)$$

reassembling,

$$S_f \cong \frac{K_m' S_m V_f}{K_f' V_m} \qquad (5b)$$

Therefore,

$$S_f \cong S_m \qquad (6a)$$

Also

$$K_f \cong \frac{V_f}{S_f} \qquad (6b)$$